Electrorheological Behavior of Side-Chain Liquid-Crystalline Polysiloxanes in Nematic Solvents

Ning Yao and Alex M. Jamieson*

Department of Macromolecular Science, Case Western Reserve University, Cleveland, Ohio 44106-7202

Received March 21, 1997; Revised Manuscript Received June 9, 1997[⊗]

ABSTRACT: The electrorheological properties of well-characterized side-chain liquid-crystalline polysiloxanes with different backbone and spacer lengths were studied in two nematic solvents: 4′-(pentyloxy)-4-biphenylcarbonitrile (5OCB), which has positive dielectric anisotropy, and *N*-(4-methoxybenzylidene)-4-butylaniline (MBBA), which has negative dielectric anisotropy. Specifically, we measured the steady-shear viscosities, η_{off} and η_{on}, in the absence and presence, respectively, of a saturation electric field. For 5OCB solutions, the electrorheological (ER) effect is positive, i.e., $\eta_{on} > \eta_{off}$. For the intrinsic viscosities, we find $[\eta_{off}] \gg [\eta_{on}]$, and $[\eta_{off}]$ shows a strong dependence on molecular weight ($[\eta_{off}] \sim M^{0.4}$) and spacer length, whereas $[\eta_{on}]$ is insensitive to the change of molecular weight and spacer length. In contrast, the ER effect of MBBA solutions is very small and slightly negative, i.e., $\eta_{on} < \eta_{off}$. In addition, $[\eta_{off}]$ and $[\eta_{on}]$ are of comparable magnitude and each shows a strong dependence on molecular weight ($[\eta_{off}] \sim [\eta_{on}] \sim M^{0.3}$). These distinctive patterns of ER behavior can be explained by a hydrodynamic model which assumes the side-chain liquid-crystalline polysiloxane has an asymmetric conformation, such that the root-mean-square end-to-end distance parallel to the director, $R_{||}$, is different from that perpendicular to the director, $R_{\perp}$. $R_{||}$ is aligned along the shear gradient in 5OCB when the field is on but is tilted toward the flow direction with the field off. In MBBA, $R_{||}$ is oriented perpendicular to the shear gradient both with the field on and with the field off.

Introduction

Upon application of an electric field transverse to the flow direction, enhanced viscosity is observed in certain fluids, which are termed electrorheological (ER) fluids.[1] Most ER fluids are colloidal dispersions of small, solid particles in insulating fluids each having different dielectric constants. A liquid to solid transition occurs when applying an electric field of requisite strength to these dispersions.[1,2] At low to moderate volume fractions, the interparticle force arising from the polarization of the particles by the applied field leads to particle agglomeration and the formation of transient chainlike structures whose size adjusts in response to the flow, fragmenting and aggregating as the shear rate increases or decreases.

Liquid-crystalline materials,[3,4] including low molar mass liquid crystals[5,6] and lyotropic solutions of stiff-chain liquid-crystalline polymers (LCPs),[7,8] may also show enhanced viscosity in an electric field. In contrast to the colloidal ER fluids, the ER effect in liquid-crystalline materials arises because of orientation of the dielectrically-anisotropic molecules by the applied field and is observed when the material has a positive dielectric anisotropy, i.e., $\Delta\epsilon = \epsilon_{||} - \epsilon_{\perp} > 0$, where $\epsilon_{||}$ and $\epsilon_{\perp}$ are the values of the dielectric constant parallel and perpendicular to the director, respectively.

It is well-known that, when a nematic liquid crystal is subject to a shear flow, the orientation response of the nematic director is determined by two of the six Leslie viscosity coefficients, α_2 and α_3.[9] Provided that α_2 is negative, a nematic material exhibits flow-aligning behavior (i.e., the director aligns at an angle close to the flow direction when $\alpha_3 < 0$) and director tumbling, with no stable alignment of the director, when $\alpha_3 > 0$. Low molar mass nematics most often show flow-aligning behavior,[9,10] unless they also have a smectic phase, when tumbling behavior may be observed in the nematic state near the transition to the smectic phase.[9,10] At low shear rates, tumbling is observed in the rheology of lyotropic stiff-chain LCP solutions.[11,12] In the presence of an electric field, lyotropic LCP solutions may show either a flow-aligning or a tumbling response, depending on the strength of the applied field, and a large viscosity increment is observed when the field is sufficiently strong.[7] If a saturation field is applied so that the director is aligned in the direction of the field, then the three Miesowicz viscosities[13] can be measured, as schematically illustrated for cone and plate geometry in Scheme 1: η_a, where the director is in the vorticity direction; η_b, where the director is in the flow direction; and η_c, where the director is in the direction of the shear gradient.[5,6]

Scheme 1. Three Miesowicz Viscosities

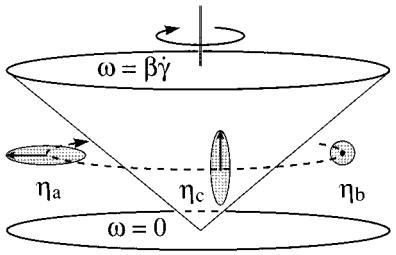

In our own work, a very large enhancement of the ER effect was observed, when a main-chain LCP was dissolved in a nematic solvent with positive $\Delta\epsilon$.[14] A much smaller enhancement was seen when a side-chain LCP of comparable molecular weight was dissolved.[15] The increased ER response of LCPs in nematic solvents arises because the LCP chain has an anisotropic conformation due to the interactions between the nematic solvent and the mesogens of the LCP, so that the root-mean-square rms end-to-end distance of the chain parallel to the director, $R_{||}$, is different from that perpendicular to the director, $R_{\perp}$. The orientation of the chain is coupled to that of the solvent molecules and

* To whom all correspondence should be addressed.
[⊗] Abstract published in *Advance ACS Abstracts,* September 1, 1997.

S0024-9297(97)00400-2 CCC: $14.00

hence changes relative to the flow direction when the electric field is applied. Thus, the dramatically different ER response[14,15] between solutions of main-chain LCPs and side-chain LCPs is explained qualitatively on the basis that, in anisotropic solvents, main-chain LCPs form a rodlike conformation ($R_{||} \gg R_{\perp}$) whereas side-chain LCPs have a quasi-spherical conformation ($R_{||} \sim R_{\perp}$), in nematic media.[14,15] A quantitative analysis of the ER response of solutions of main-chain LCPs in nematic solvents can be achieved[14] within the framework of a theoretical model developed by Brochard,[16] assuming that the viscosity η_{on} is equivalent to the Miesowicz viscosity η_c, while η_{off} is numerically close to the Miesowicz viscosity η_b. Thus, our observation[14] that, for main-chain LCPs, the intrinsic viscosity $[\eta_{on}] \gg [\eta_{off}]$ is consistent with the prediction[16] that the ratio of the viscosity increments $\delta\eta_c/\delta\eta_b = R_{||}^4/R_{\perp}^4$. Depending upon the flexibility of the chain backbone and the lengths and density of the spacer groups which link the mesogens to the backbone, the conformation of side-chain LCPs may be slightly prolate or slightly oblate,[17] which should lead to quite different ER responses. A further complication in the rheological behavior of nematic solutions of side-chain LCPs is the observation that, at sufficiently high concentrations, such solutions show director-tumbling behavior even if the solvent is flow aligning.[18]

In this work, side-chain liquid-crystalline polysiloxanes with different backbone and spacer lengths were synthesized. The ER behavior was investigated in two solvents: 4′-(pentyloxy)-4-biphenylcarbonitrile (5OCB, T_{N-I} = 67 °C), which has positive $\Delta\epsilon$, and *N*-(4-methoxybenzylidene)-4-butylaniline (MBBA, T_{N-I} = 40 °C), which has negative $\Delta\epsilon$. The viscosities η_{on} and η_{off} were measured as a function of concentration, temperature, molecular weight, side-chain density, and spacer length. The results, which contrast sharply with our earlier results on the viscosities of nematic solutions of main-chain LCPs, are discussed in terms of the Brochard model.[16]

Experimental Section

Materials. Toluene was distilled over sodium under nitrogen just before use. Tetrahydrofuran (THF) was distilled from the blue mixture of THF, benzophenone, and sodium under nitrogen just before use. Pyridine was distilled over calcium hydride and stored over 4 Å molecular sieves. 5OCB, MBBA, dichloromethylsilane, ethyl ether, hexamethyldisiloxane, trifluoromethanesulfonic acid, hydrogen hexachloroplatinate(IV) hydrate, 4-hydroxybenzoic acid, thionyl chloride, 4-methoxyphenol, allyl bromide, 5-bromo-1-pentene, phosphorus tribromide, ω-undecylenyl alcohol, potassium hydroxide, potassium iodide, ethanol, and hydrochloric acid were used as received.

Analytical Methods. ^{1}H-NMR spectra were taken using a Varian XL-200 200-MHz FT NMR spectrometer. Chemical shifts (δ) were given in ppm with the peak (7.27 ppm) of $CHCl_3$ as reference. GPC experiments were carried out on a Waters chromatograph connected to a Waters 410 differential refractometer with polystyrene as standards in THF. ER measurements were performed on a Carri-Med controlled-stress rheometer using cone and plate fixtures (cone angle = 0.5°, cone radius = 10 mm) as electrodes. A voltage of 100 V was applied to the cone through mercury by a Bertan Model 215 high-voltage power supply. With a gap of 15 μm, the resulting electric field is about 6.7 kV/mm at the tip and 1.1 kV/mm at the edge. Previous work[14,15] has established that this represents a saturation field level at which full alignment of the director is maintained for several nematic solvents in steady flow over a wide range of shear rates, so that the Miesowicz viscosity η_c is measured. Under these conditions, for nematic LCP solutions of high viscosity, η_c can be obtained by extrapolation to zero shear.[14,15] The sample temperature was controlled accurately to 0.1 °C.

Scheme 2. Synthesis of Side-Chain Liquid-Crystalline Polysiloxanes

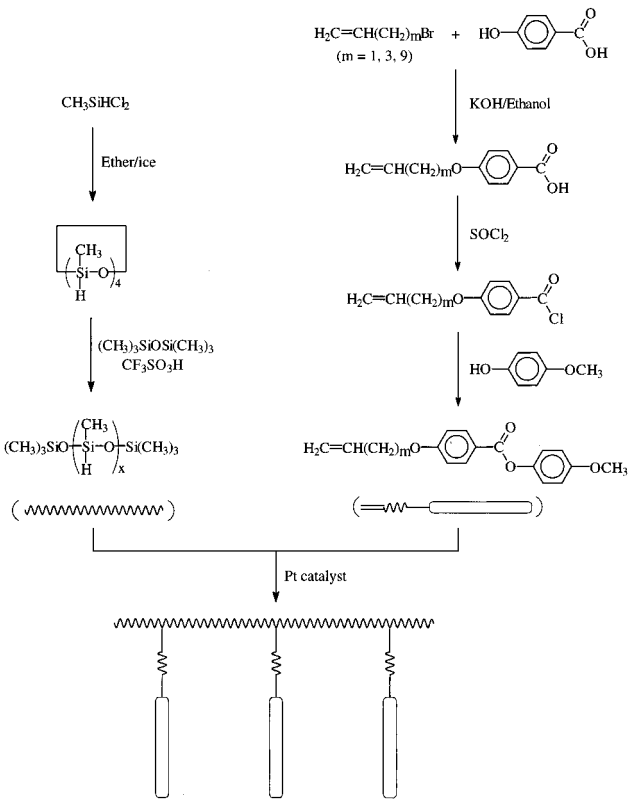

Synthesis of Side-Chain Liquid-Crystalline Polysiloxanes. The synthesis of side-chain liquid-crystalline polysiloxanes is outlined in Scheme 2. The Pt catalyst, dicyclopentadienylplatinum(II) chloride,[19] and 11-bromo-1-undecene[20] were prepared based on literature procedures.

A. 1,3,5,7-Tetramethylcyclotetrasiloxane (D_4H).[21] Dichloromethylsilane (110 mL, 1.05 mol) was added with vigorous stirring to a mixture of 250 mL of ethyl ether and 500 g of ice over 0.5 h. After stirring an additional 0.5 h, the organic phase was separated, washed with water until pH = 7, and dried over sodium sulfate. The ether was then removed, and distillation of the residue at 133−136 °C gave a cloudy liquid. Redistillation of the cloudy liquid over calcium hydride gave 20 g of clear liquid (yield: 32%). ^{1}H-NMR ($CDCl_3$): δ 4.69 (q, 1H, SiH), 0.16 (d, 3H, CH_3).

B. 4-(Allyloxy)benzoic Acid (1), 4-(Pentenyloxy)benzoic Acid (2), and 4-(Undecenyloxy)benzoic Acid (3). All three compounds were prepared by similar methods. The synthesis of compound **2** is described below. 4-Hydroxybenzoic acid (7.5 g, 54 mmol) was added to a solution of 7.9 g of potassium hydroxide (85%) in 300 mL of ethanol. Potassium iodine (0.1 g) was then added, and the solution was heated to reflux temperature. After slow addition of 5-bromo-1-pentene (8.0 g, 54 mmol), the resulting solution was refluxed overnight. A total of 150 mL of solvent was then removed by distillation. The remaining mixture was cooled, poured into 500 mL of water, and acidified with 6 N aqueous hydrochloric acid. The precipitate was filtered, washed with water, and recrystallized from ethanol to give 4.8 g of crystalline compound.

Compound 1. ^{1}H-NMR ($CDCl_3$): δ 11−12 (b, 1H, COOH), 8.09−6.93 (dd, 4H, C_6H_4), 6.05 (m, 1H, =CH), 5.48 (dd, 2H, $=CH_2$), 4.61 (d, 2H, CH_2).

Compound 2. ^{1}H-NMR ($CDCl_3$): δ 11−12 (b, 1H, COOH), 8.09−6.92 (dd, 4H, C_6H_4), 5.86 (m, 1H, =CH), 5.04 (dd, 2H, $=CH_2$), 4.04 (t, 3H, CH_2), 2.26 (m, 2H, CH_2), 1.92 (m, 2H, CH_2).

Compound 3. ^{1}H-NMR ($CDCl_3$): δ 11−12 (b, 1H, COOH), 8.09−6.95 (dd, 4H, C_6H_4), 5.84 (m, 1H, =CH), 4.92 (dd, 2H, $=CH_2$), 4.10 (t, 2H, CH_2), 2.04 (m, 2H, CH_2), 1.84 (m, 2H, CH_2), 1.33 (m, 12H, CH_2).

C. 4-[(Allyloxy)benzoyl] 4′-Methoxyphenyl Ether (4), 4-[(Pentenyloxy)benzoyl] 4′-Methoxyphenyl Ether (5), and 4-[(Undecenyloxy)benzoyl] 4′-Methoxyphenyl Ether (6). All three compounds were prepared by similar methods. The synthesis of compound **5** is described below. A mixture of 4-(pentenyloxy)benzoic acid (4.8 g, 21.4 mmol), thionyl chloride (10 mL), and *N*,*N*-dimethylformamide (2 drops) was stirred overnight under nitrogen at room temperature. The excess thionyl chloride was then removed under reduced pressure. Distillation of the remaining liquid at 143 °C/5 mmHg gave 4.5 g of liquid. The liquid was dissolved in 20 mL of THF containing 4 mL of pyridine. The resulting solution was added into 50 mL of a THF solution containing 2.45 g of 4-methoxyphenol and 3 mL of pyridine. The mixture was stirred at room temperature for 8 h. Then 40 mL of THF was removed. The remaining mixture was poured into 100 mL of water. The resulting precipitate was filtered, washed with water, and recrystallized from ethanol twice to give 4.5 g of a crystalline compound.

Compound 4. ^{1}H-NMR ($CDCl_3$): δ 8.18−7.02 (dd, 4H, C_6H_4), 6.99−6.92 (dd, 4H, C_6H_4), 6.03 (m, 1H, =CH), 5.38 (dd, 2H, $=CH_2$), 4.65 (d, 2H, CH_2), 3.84 (s, 3H, CH_3).

Compound 5. ^{1}H-NMR ($CDCl_3$): δ 8.15−7.13 (dd, 4H, C_6H_4), 7.10−6.91 (dd, 4H, C_6H_4), 5.85 (m, 1H, =CH), 5.04 (dd, 2H, $=CH_2$), 4.06 (t, 2H, CH_2), 3.82 (s, 3H, CH_3), 2.25 (m, 2H, CH_2), 1.92 (m, 2H, CH_2).

Compound 6. ^{1}H-NMR ($CDCl_3$): δ 8.16−7.14 (dd, 4H, C_6H_4), 7.12−6.91 (dd, 4H, C_6H_4), 5.81 (m, 1H, =CH), 4.97 (dd, 2H, $=CH_2$), 4.04 (t, 2H, CH_2), 3.83 (s, 3H, CH_3), 2.04 (m, 2H, CH_2), 1.83 (m, 2H, CH_2), 1.33 (m, 12H, CH_2).

D. Poly(methylhydrosiloxane) (PMHS). Poly(methylhydrosiloxane)[22] was prepared using a modified procedure. D_4H (3.18 g, 53 mmol), hexamethyldisiloxane (0.30 mL, 1.4 mmol), and trifluoromethanesulfonic acid (0.02 mL) was stirred under nitrogen at room temperature for 24 h. A total of 40 mL of ethyl ether was added, and the resulting solution was washed with water until pH = 7. The ether layer was dried over sodium sulfate and distilled under reduced pressure. The residue was then purified under vacuum at 150 °C for 24 h to give a clear liquid. ^{1}H-NMR ($CDCl_3$): δ 4.72 (q, SiH), 0.20 (d, CH_3), 0.12 (s, CH_3).

E. Side-Chain Liquid-Crystalline Polysiloxane. The olefinic derivative (0.5 g, 10 mol % excess versus the SiH groups in PMHS) was dissolved in 25 mL of dry, freshly distilled toluene containing an appropriate amount of PMHS. The reaction mixture was heated to 110 °C under nitrogen, and 50 μg of dicyclopentadienylplatinum(II) chloride was then added as a solution in THF (0.2 mg/mL). The resulting solution was kept at 110 °C under nitrogen for 24 h. After the solution was cooled, excess methanol was added into the solution and the polymer was collected by centrifugation at 2000 rpm for 1 h. After reprecipitating the polymer two more times from THF, the polymer was dissolved in THF and filtered through a 0.2 μm filter. The solvent was slowly removed at 50 °C, and the polymer was then dried thoroughly in vacuo at 75 °C for 24 h.

Results

Synthesis of Side-Chain Liquid-Crystalline Polysiloxanes. Equilibration polymerization of cyclic siloxanes is an effective route to the preparation of polysiloxanes with controlled molecular weight and functionality.[23] With trifluoromethanesulfonic acid as catalyst and hexamethyldisiloxane as end capper, the equilibration polymerization of D_4H gave PMHS as a viscous liquid. The average molecular weight of the polymer was controlled by adjusting the relative mole ratio of D_4H to hexamethyldisiloxane. Based on end-group analysis of the ^{1}H-NMR results (Figure 1), the number-average degree of polymerization (DP) of the PMHS was calculated using the equation

$$\mathrm{DP} = [(I_a + I_b)/3]/(I_c/18) \quad (1)$$

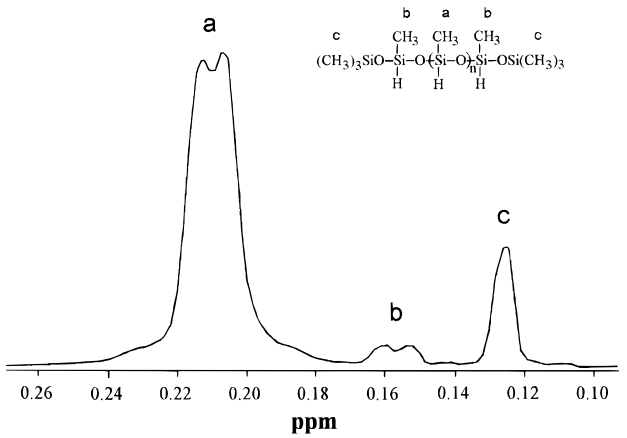

Figure 1. ^{1}H-NMR spectrum ($CDCl_3$) of the poly(methylhydrosiloxane).

Table 1. Molecular Weights of Fully-Hydrosilated Side-Chain Liquid-Crystalline Polysiloxanes

no.	DP[a]	n[b]	M_n	M_w	M_w/M_n
1	45	3	9 600	13 500	1.41
2	72	3	11 800	22 200	1.88
3	127	3	14 100	26 000	1.84
4	198	3	16 600	40 300	2.42
5	45	5	7 900	9 700	1.23
6	72	5	9 700	12 300	1.27
7	127	5	10 500	17 800	1.69
8	198	5	12 400	21 200	1.71
9	45	11	9 800	11 500	1.17
10	72	11	9 700	14 000	1.44
11	127	11	11 700	22 100	1.89
12	198	11	13 100	33 300	2.54

[a] DP = degree of polymerization of the backbones based on ^{1}H-NMR analysis. [b] n = spacer length of the side chains.

Table 2. Molecular Weights of Partially-Hydrosilated Side-Chain Liquid-Crystalline Polysiloxanes

no.	DP[a]	n[b]	SiH content (%)[c]	M_n	M_w	M_w/M_n
12	198	11	<5	13 100	33 300	2.54
13	198	11	16	11 000	24 100	2.19
14	198	11	32	8 800	14 300	1.62
15	198	11	73	6 900	13 100	1.90

[a] DP = degree of polymerization of the backbones based on ^{1}H-NMR analysis. [b] n = spacer length of the side chains. [c] Percentage of unhydrosilated SiH.

in which $I_a + I_b$ is the total intensity of the methyl resonances from the repeat units of PMHS and I_c is the intensity of the methyl resonance from the PMHS end groups (Figure 1). The DP values obtained in this way are listed in Table 1 and were used to estimate the average backbone lengths of the side-chain liquid-crystalline polysiloxanes.

Using a suitable Pt catalyst, the SiH groups of PMHS may react with vinyl compounds to high degrees of conversion.[24] In this work, dicyclopentadienylplatinum(II) chloride[19] was chosen as catalyst in order to obtain colorless products. The side-chain liquid-crystalline polysiloxanes synthesized in this work can show either a nematic phase, a smectic phase, or both depending upon the spacer length.[19,25,26] Three side-chain precursors with spacer lengths n = 3, 5, and 11, respectively, were used for the hydrosilation reactions as shown in Scheme 2. Note that the absolute molecular weights of the samples with the same backbone length should increase as the spacer length increases. The results of GPC analysis of the side-chain LCPs (Tables 1 and 2) show that the polydispersities of most samples are less

Scheme 3. Structures of Nematic Solvents

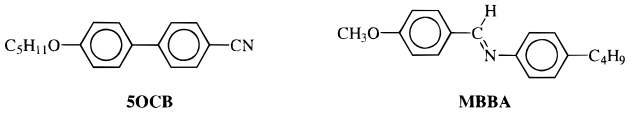

5OCB **MBBA**

than 2 and decrease as the backbone length decreases. For fully-hydrosilated samples with the same backbone length, the GPC molecular weights relative to the polystyrene standards in THF have their highest values when $n = 3$ and their lowest values when $n = 5$. For partially-hydrosilated samples with the same backbone length, the GPC molecular weight decreases as the amount of unhydrosilated SiH increases. Obviously, the fully-hydrosilated samples with different spacer lengths have different hydrodynamic behaviors in THF, the hydrodynamic volume being largest for $n = 3$ and smallest for $n = 5$. We conclude that there is some conformational rigidity in the polymer having $n = 3$ compared to that with $n = 5$ and that the increase in volume on going from $n = 5$ to $n = 11$ comes from the increase in spacer length.

ER Behavior of 5OCB and MBBA. 5OCB is a linear molecule whose dipole direction is coaxial with its molecular axis (Scheme 3). As a result, the molecule of 5OCB has a positive $\Delta\epsilon$ and will line up parallel to the electric field when a sufficiently high voltage is applied. MBBA is also a linear molecule (Scheme 3) but its dipole is at an angle to the molecular axis and the $\Delta\epsilon$ of this material is negative. The effect of a strong electric field on MBBA is to align the director perpendicular to the field.

The shear rate dependence of the viscosities of 5OCB and MBBA are shown in Figures 2 and 3. Two viscosities, η_{off} and η_{on}, were measured, η_{off} referring to the viscosity determined with the electric field off and η_{on} referring to the viscosity determined with the electric field on. The results in Figures 2 and 3 indicate that, in the nematic state under steady flow conditions, as expected, 5OCB ($T = 62$ °C) shows a positive ER effect, i.e., $\eta_{on} > \eta_{off}$, whereas MBBA ($T = 30$ °C) does not show a measurable ER effect. 5OCB, a flow-aligning nematic with positive $\Delta\epsilon$, has its director parallel to the flow with the field off and perpendicular to the flow with the field on; MBBA, a flow-aligning nematic with negative $\Delta\epsilon$, has its director parallel to the flow both with the field on and with the field off. The small positive ER effect observed for MBBA in the low shear rate region is not understood at present. Possibly, an additional viscous force is required to produce uniform flow alignment during start-up flow due to differences in texture of the unsheared sample in the presence of an applied field. Note that, since the Miesowicz viscosities of MBBA are known, we can confirm the expectation that $\eta_{off} = \eta_{on} \approx \eta_b$ for MBBA. Thus, from Figure 3, we determine $\eta_b = 0.20$ P at $T = 30$ °C, compared to literature value[27] of $\eta_b = 0.19$ P. In our previous paper,[14] it was shown for several low molar mass nematics that the measured values of η_{off} and η_{on} were numerically in agreement with literature values of η_b and η_c, respectively.

ER Behavior of Side-Chain Liquid-Crystalline Polysiloxanes in 5OCB and MBBA. When a small amount of LCP is dissolved in a nematic solvent, just as for isotropic polymer solutions, a large change in rheological behavior occurs because the polymer chain occupies a large hydrodynamic volume fraction in the nematic medium. Also, the interaction between the anisotropic solvent and the mesogens of the LCP makes

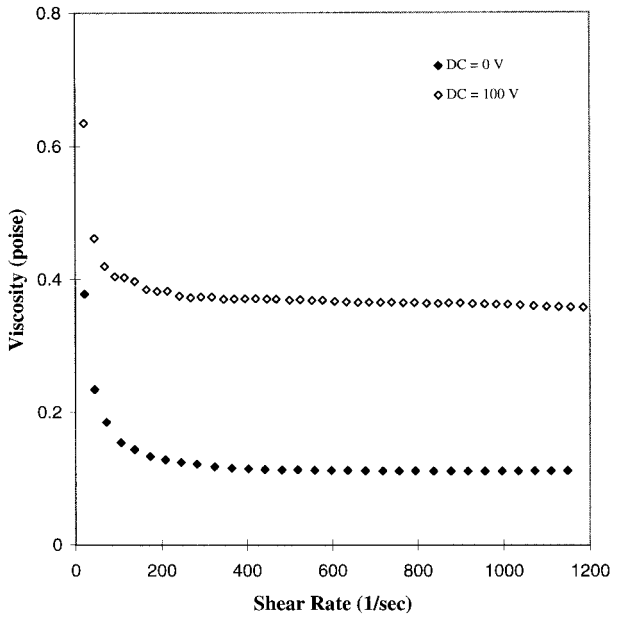

Figure 2. Shear rate dependence of the viscosities of pure 5OCB.

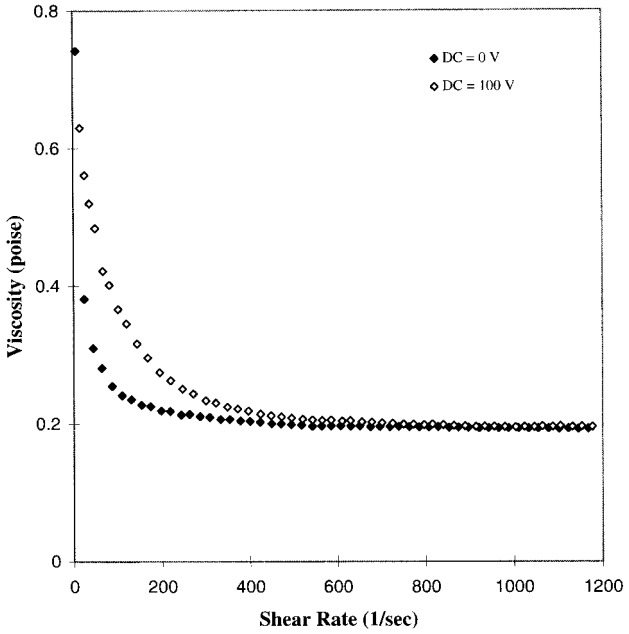

Figure 3. Shear rate dependence of the viscosities of pure MBBA.

the polymer conformation nonspherical. Theoretical analysis[16] of the viscosity increments due to the dissolution of flexible polymer chains in a nematic fluid indicates that the viscosity increments depend on the ratio of $R_{||}$ and $R_{\perp}$, the rms end-to-end distances of the polymer chain parallel and perpendicular to the director **n** (Scheme 4). The orientation of the nonspherical polymer chain under the influence of an applied electric field will therefore strongly influence the viscosities of nematic solutions of LCPs.

Figure 4 shows the viscosity curves of a side-chain LCP (DP = 45, $n = 3$, $c = 0.087$ g/mL) in 5OCB. As for the pure solvent (Figure 2), a positive ER effect is observed in the nematic phase ($T = 62$ °C). On comparison of Figures 2 and 4, it is apparent that η_{off} and η_{on} have increased on addition of the LCP, with the largest percentage increase occurring for η_{off}. As we will discuss later, this indicates that in the presence of the

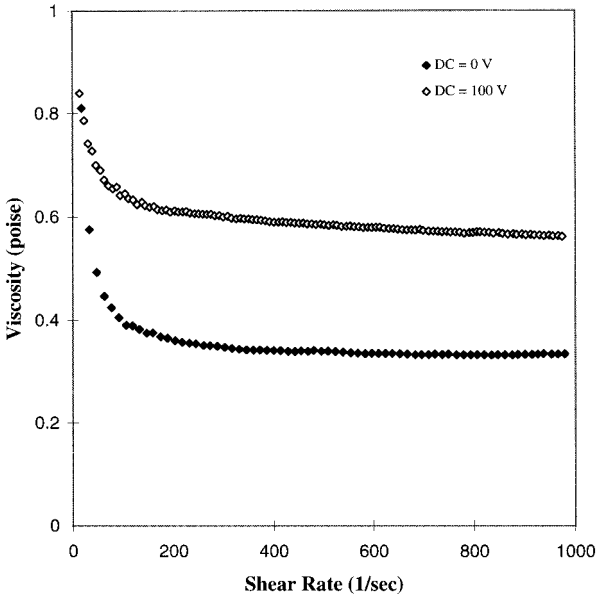

Figure 4. Shear rate dependence of the viscosities of the side-chain liquid-crystalline polysiloxane in 5OCB (DP = 45, n = 3, c = 0.087 g/mL).

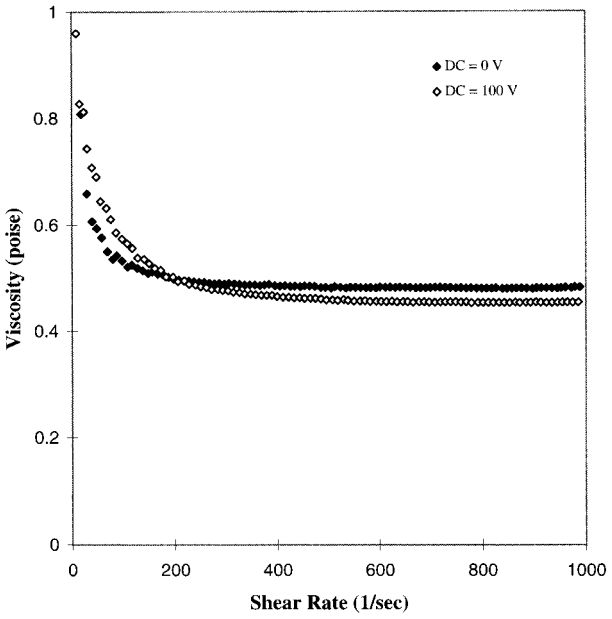

Figure 5. Shear rate dependence of the viscosities of the side-chain liquid-crystalline polysiloxane in MBBA (DP = 198, n = 3, c = 0.043 g/mL).

Scheme 4. Conformations of a Side-Chain LCP

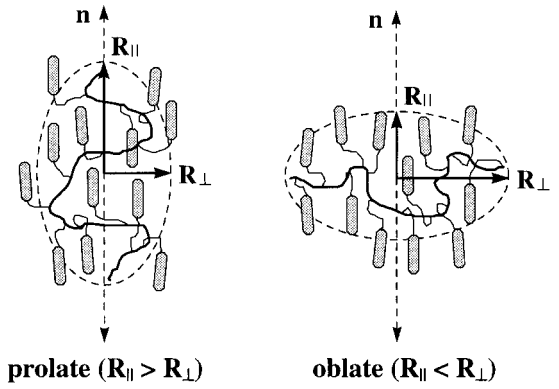

field the effective hydrodynamic volume is smaller than that in the absence of the field. When 5OCB was replaced with MBBA, as shown in Figure 5, in the nematic phase under steady flow conditions, η_{on} is smaller than η_{off}; i.e., there is a small negative ER effect. Also, it is apparent, comparing Figures 3 and 5, that the increase in both η_{on} and η_{off} is of comparable magnitude, though slightly smaller in the former. Thus, the effective hydrodynamic volume of the LCP is slightly smaller with the field on than with the field off.

Concentration Dependence of Viscosities. Figures 6 and 7 show the concentration dependence of the viscosities of the side-chain LCP having DP = 198 and n = 3 in 5OCB and in MBBA, respectively. Linear dependences of η_{off} and η_{on} on concentration were observed for both 5OCB and MBBA in dilute solution. Figure 6 indicates that the concentration dependence is stronger in the nematic state with the field off than with the field on. Specifically, it can be clearly seen in Figure 6 that $\Delta\eta = \eta_{on} - \eta_{off}$ becomes increasingly smaller at T = 62 and 67 °C as LCP is added to the solution. In the isotropic state (T = 82 °C), the concentration dependence is comparable to that of η_{on} in the nematic state and is unaffected by the field, as expected. Figure 7 shows that the concentration dependence of the same polymer in MBBA is very similar for η_{off} and η_{on} in both the nematic and isotropic states,

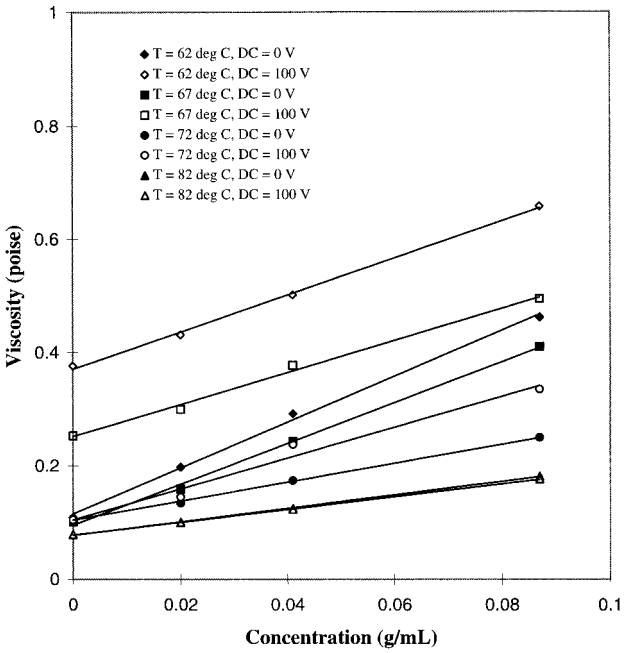

Figure 6. Concentration dependence of the viscosities of the side-chain liquid-crystalline polysiloxane in 5OCB (DP = 198, n = 3).

although it is again stronger in the nematic state. These observations can be quantified in terms of the intrinsic viscosities, $[\eta_{off}]$ and $[\eta_{on}]$, defined in the usual way. Specifically, in 5OCB, $[\eta_{off}]$ is larger in the nematic state than $[\eta_{on}]$, which is comparable to the isotropic value, $[\eta_{iso}]$. This situation is the reverse of that found for main-chain LCP solutions, where $[\eta_{on}] \gg [\eta_{off}] \sim [\eta_{iso}]$.[14] In MBBA, $[\eta_{off}]$ is only slightly larger than $[\eta_{on}]$ in the nematic state, and each is substantially larger than $[\eta_{iso}]$. If we assume that $[\eta] = 2.5N_A V_h^{eff}/M$, where N_A is Avogadro's number, V_h^{eff} is the effective hydrodynamic volume of the polymer, and M is polymer molecular weight, it follows that these variations in intrinsic viscosity can be related to corresponding differences in the effective hydrodynamic volume. One point to make regarding Figure 6 is that, in common

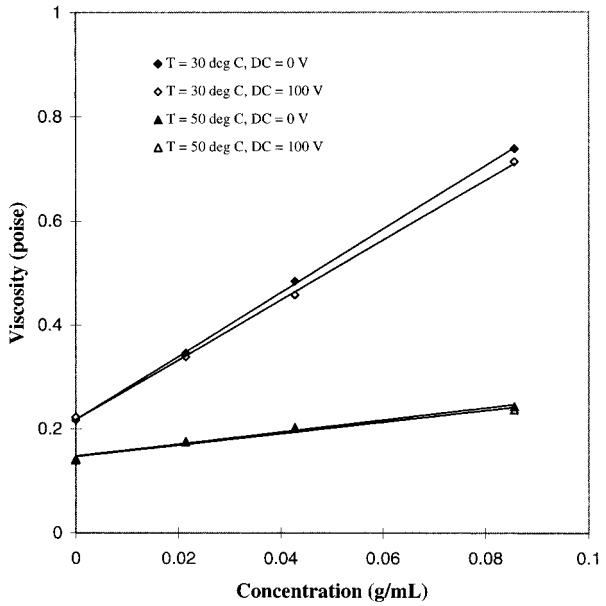

Figure 7. Concentration dependence of the viscosities of the side-chain liquid-crystalline polysiloxane in MBBA (DP = 198, $n = 3$).

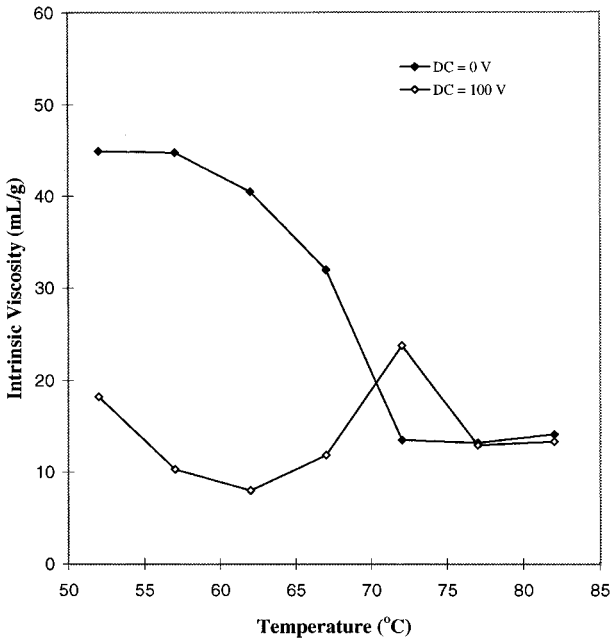

Figure 8. Temperature dependence of the intrinsic viscosities of the side-chain liquid-crystalline polysiloxane in 5OCB (DP = 198, $n = 3$).

with octylcyanobiphenyl,[18] 5OCB has a slightly higher viscosity in the isotropic state than in the nematic state just below T_{N-I}. This is also true for MBBA.

Temperature Dependence of Intrinsic Viscosities. As temperature increases, the order parameters of both the side-chain LCPs and the nematic solvents will decrease. At higher temperatures, the interaction between the mesogens in a side-chain LCP and a nematic solvent becomes weaker. As a result, the conformation of the side-chain LCP may become less anisotropic and the intrinsic viscosities $[\eta_{off}]$ and $[\eta_{on}]$ can be expected to decrease with increasing temperature and become similar near the transition temperature, T_{N-I}. The observed behavior is shown in Figures 8 and 9 for 5OCB and MBBA solutions, respectively. For the polymer of DP = 198, $n = 3$, in 5OCB, at lower

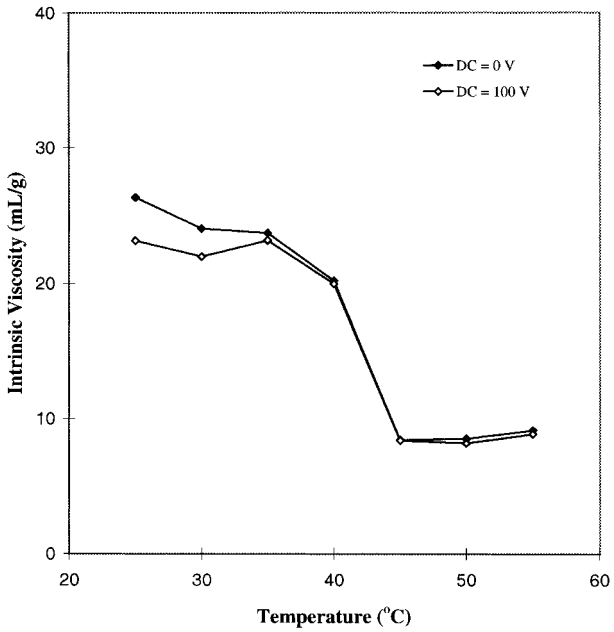

Figure 9. Temperature dependence of the intrinsic viscosities of the side-chain liquid-crystalline polysiloxane in MBBA (DP = 198, $n = 3$).

temperatures in the nematic state, $[\eta_{off}] > [\eta_{on}]$, and each decreases initially as temperature is raised. Thus, the effective hydrodynamic volume with the field on is much smaller than that with the field off. Microscopic examination indicates that a biphasic transition region exists in the temperature range $T = 68-75$ °C, slightly higher than the transition temperature of pure 5OCB ($T_{N-I} = 67$ °C). As the temperature approaches T_{N-I}, $[\eta_{on}]$ begins to increase and, in the biphasic region at $T = 72$ °C, actually becomes larger than $[\eta_{off}]$. Recall, however, that at 72 °C the pure solvent 5OCB is in the isotropic state and has a relatively high viscosity (Figure 6). In the isotropic state $[\eta_{off}]$ and $[\eta_{on}]$ are identical and weakly dependent on temperature, as expected.

For the same polymer in MBBA, $[\eta_{on}]$ is only slightly lower than $[\eta_{off}]$, indicating that the effective hydrodynamic volume is slightly smaller with the field on. Both $[\eta_{off}]$ and $[\eta_{on}]$ decrease with temperature. A shoulder is evident at 35 °C in $[\eta_{on}]$ which becomes comparable to $[\eta_{off}]$. Microscopic examination indicates that a biphasic transition region exists in the temperature range $T = 30-35$ °C, i.e., slightly below the transition temperature of pure MBBA ($T_{N-I} = 40$ °C). The shoulder in $[\eta_{on}]$ at $T = 35$ °C is partly due to the higher viscosity of the solvent in the isotropic state. At higher temperatures, $[\eta_{off}]$ and $[\eta_{on}]$ each decrease to smaller values characteristic of the isotropic solution. Later, we discuss these results in the context of the Brochard theory,[16] but here we note that the above observations in 5OCB can be interpreted, if the LCP conformation is assumed to be ellipsoidal, such that with the field on the chain dimension $R_{||}$ is aligned in the direction of the shear gradient and is perpendicular to the shear gradient with the field off. In MBBA, the $R_{||}$ is perpendicular to the shear gradient both with the field on and with the field off.

Molecular Weight Dependence of Intrinsic Viscosities. When PMHSs with different DP values are used for hydrosilation, side-chain LCPs with the same spacer length but different backbone lengths can be obtained. In Figure 10, the molecular weight depen-

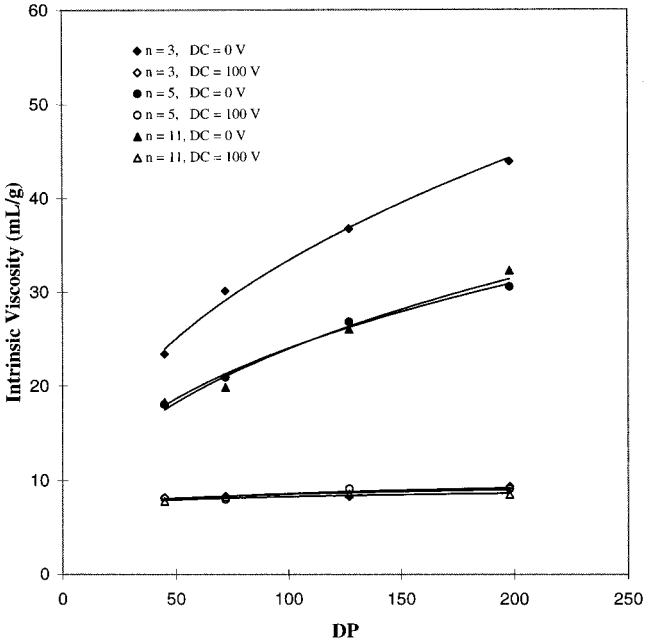

Figure 10. DP dependence of the intrinsic viscosities of the side-chain liquid-crystalline polysiloxanes in 5OCB (T = 57 °C).

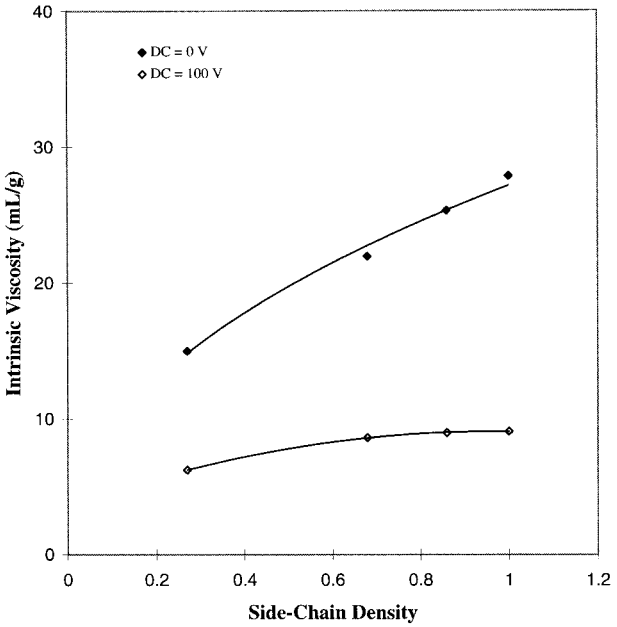

Figure 11. Side-chain density (normalized to fully-hydrosilated LCP) dependence of the intrinsic viscosities of the side-chain liquid-crystalline polysiloxanes in 5OCB (T = 62 °C, DP = 198, n = 11).

dence of $[\eta_{off}]$ and $[\eta_{on}]$ for each polymer, at fixed spacer length n = 3, 5, and 11, is shown in 5OCB at T = 57 °C in the nematic state. Evidently, for each species, $[\eta_{off}] \gg [\eta_{on}]$, and we observe that, while $[\eta_{off}]$ has a substantial molecular weight dependence ($[\eta_{off}] \sim M^{0.4}$), $[\eta_{on}]$ is remarkably insensitive to molecular weight ($[\eta_{on}] \sim M^{0.1}$). Note that these exponents are smaller than that of a linear random coil (0.5−0.6), presumably reflective of the side-chain architecture. These results contrast sharply with our previous observations for main-chain LCPs, where $[\eta_{off}] \ll [\eta_{on}]$ and $[\eta_{on}]$ is strongly molecular weight dependent ($[\eta_{on}] \sim M$).[14] Also apparent in Figure 10, $[\eta_{off}]$ is significantly larger for n = 3 than for n = 5 and n = 11, but the difference disappears for $[\eta_{on}]$. Further discussion of the spacer length dependence of the intrinsic viscosities will be given below. When the LCP molecular weight was changed by varying the side-chain density on the same polysiloxane backbone (DP = 198, n = 11), a similar result was obtained (Figure 11). Comparing Figures 10 and 11, we see that $[\eta_{off}]$ has a strong dependence on side-chain density comparable to that on backbone length. This dependence, however, is largely eliminated by the application of the electric field. The $[\eta_{on}]$ values for fully-hydrosilated LCPs in Figure 11 are only slightly larger than those for the partially-hydrosilated polymers.

When 5OCB is replaced with MBBA, a quite different pattern of viscometric behavior was observed (Figure 12). In this case, in the nematic state at T = 25 °C, the value of $[\eta_{on}]$ is comparable to, though slightly smaller than, that of $[\eta_{off}]$, and both $[\eta_{off}]$ and $[\eta_{on}]$ have a similar dependence on molecular weight ($[\eta_{off}] \sim [\eta_{on}] \sim M^{0.3}$). Again the exponent is significantly smaller than that for a random coil. In the isotropic state, $[\eta_{on}]$ is indistinguishable from $[\eta_{off}]$, as expected. We will shortly discuss these results in the context of the Brochard theory but point out here again that our observations can be rationalized if the LCP is assumed to have an ellipsoidal conformation in the nematic state. In 5OCB, which has positive $\Delta\epsilon$, a viscosity decrease is observed because the chain dimension $R_{||}$ becomes aligned with the shear gradient when the field is switched on. In MBBA, which has negative $\Delta\epsilon$, little change in viscosity occurs because $R_{||}$ is tilted from the shear gradient both with the field on and with the field off.

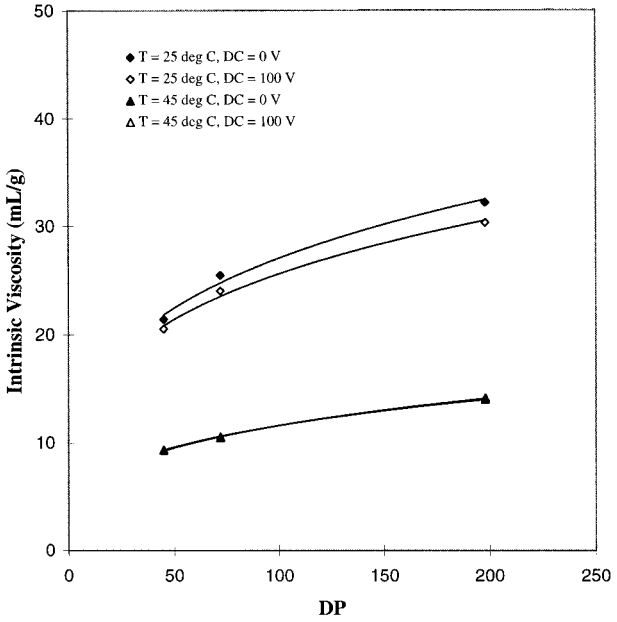

Figure 12. Molecular weight dependence of the intrinsic viscosities of the side-chain liquid-crystalline polysiloxanes in MBBA (n = 3).

Spacer Length Dependence of Intrinsic Viscosities. When the backbone length and the side-chain density are kept constant, the intrinsic viscosities of side-chain LCPs with different spacer lengths are expected to be sensitive to the coupling between the mesogens and the backbone. Figure 13 shows the spacer length dependence of the intrinsic viscosities of side-chain LCPs with DP = 45, 72, 127, and 198 and spacer lengths n = 3, 5, and 11, in 5OCB. In the absence of the electric field, $[\eta_{off}]$ decreases for all four molecular weights as the spacer length increases from 3 to 5 and then $[\eta_{off}]$ increases slightly when the spacer

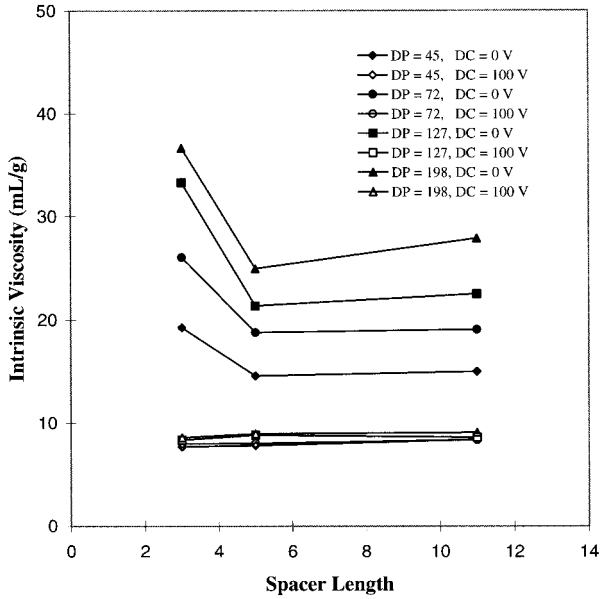

Figure 13. Spacer length dependence of the intrinsic viscosities of the side-chain liquid-crystalline polysiloxanes in 5OCB (T = 62 °C).

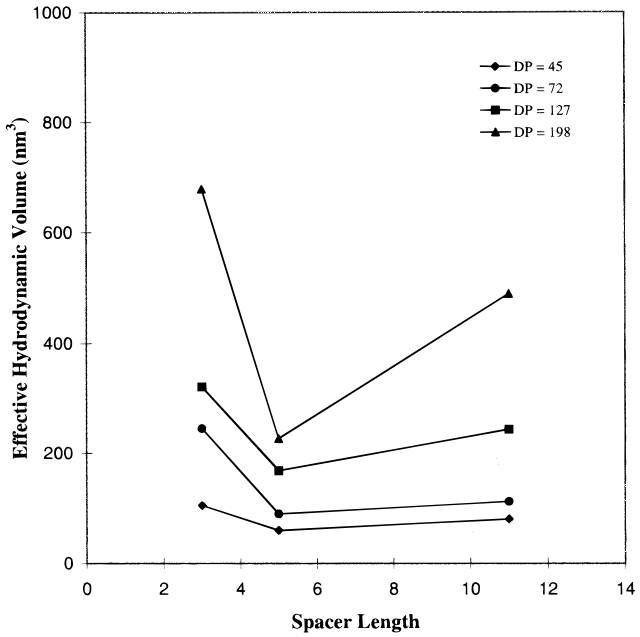

Figure 14. Spacer length dependence of the effective hydrodynamic volumes of the side-chain liquid-crystalline polysiloxanes in THF (T = 30 °C).

length increases from 5 to 11. As demonstrated in Figures 14 and 15, these results are consistent with the GPC data in Table 1. Figure 14 shows values of the LCP hydrodynamic volume, V_h^{eff}, in THF computed from the GPC molecular weight values relative to polystyrene standards, via the Mark−Houwink relation of Appelt and Meyerhoff.[28] Figure 15 shows the corresponding V_h^{eff} values in the nematic state computed from $[\eta_{off}]$ and the number-average molecular weights estimated from NMR data. Evidently, in each case, the LCP specimens with $n = 5$ have the smallest V_h^{eff}. The decrease in V_h^{eff} from $n = 3$ to 5 apparently reflects the better decoupling of side-chain and backbone orientation with the longer spacer; the increase in V_h^{eff} from $n = 5$ to 11 presumably arises from the additional volume contributed by the longer spacer.

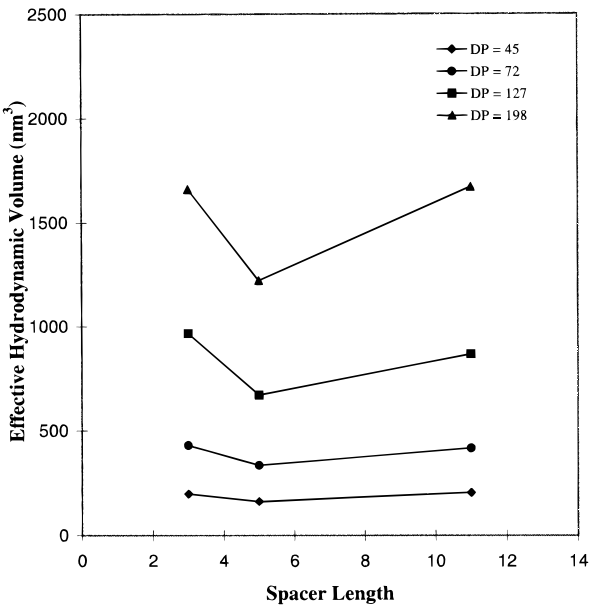

Figure 15. Spacer length dependence of the effective hydrodynamic volumes of the side-chain liquid-crystalline polysiloxanes in 5OCB (T = 62 °C).

Discussion

In the case of nematic solutions of main-chain LCPs, a quantitative interpretation was achieved[14] using the hydrodynamic model described by Brochard.[16] This was possible because these solutions exhibit flow-aligning behavior, and we could make the assignments $[\eta_{off}] \sim [\eta_b]$ and $[\eta_{on}] = [\eta_c]$, where $[\eta_b]$ and $[\eta_c]$ are two of the Miesowicz viscosities. For side-chain LCPs, a potential problem arises in interpreting $[\eta_{off}]$ since our previous rheological studies[18] show that nematic solutions of side-chain LCPs, at sufficiently high LCP concentration, may have positive values of the Leslie viscosity α_3 and hence exhibit director-tumbling behavior even if the solvent is flow-aligning ($\alpha_3 < 0$), as indeed predicted by the Brochard model.[16] Experimental observation[10,29] and computer simulation[30] suggests that for such materials, under steady flow, the nematic director tends to move out of the shear plane toward the vorticity axis, creating defects in steady flow, and so the viscosity measured is not well-defined. Experimentally, however, for tumbling low molar mass nematics, the measured steady-shear viscosity remains small,[31] numerically comparable to the Miesowicz viscosity η_a. On the other hand, if the LCP concentration is low, the solution remains flow-aligning and the measured viscosity is close to η_b. Since the determination of the intrinsic viscosity involves extrapolation to zero concentration, we assume in our discussion below $[\eta_{off}] \sim [\eta_b]$.

In the presence of a strong electric field, for a nematic with positive $\Delta\epsilon$, theory[5] and experiment[6] indicate that the tumbling phenomenon is suppressed and so we can safely make the assignment $[\eta_{on}] = [\eta_c]$, for solutions in 5OCB. For a nematic with negative $\Delta\epsilon$ and positive α_3, it has been suggested that, at high shear rates, the electric torque may act either to destabilize[5] or stabilize[32] the director to out-of-plane fluctuations. Note that, to our knowledge, no low molar mass nematic with negative $\Delta\epsilon$ and $\alpha_3 > 0$ is known, and so there is no experimental precedent to choose between these two alternatives. It is clear that the director will tend to locate in the plane formed by the flow direction and the vorticity axis, and since the change in viscosity on

Table 3. Hydrodynamic Parameters of Fully-Hydrosilated Side-Chain Liquid-Crystalline Polysiloxanes in 5OCB (T = 62 °C)

no.	DP[a]	n[b]	$\eta°[\eta_{off}]$ (P·mL/g)	$\eta°[\eta_{on}]$ (P·mL/g)	$R_{\|}/R_{\perp}$	τ_r (μs)	$R_{h,off}$ (nm)	$R_{h,on}$ (nm)
1	45	3	2.092	2.899	1.08	1.37	3.62 (3.73)[c]	2.66 (3.69)
2	72	3	2.828	3.010	1.02	2.60	4.68 (4.64)	3.16 (4.55)
3	127	3	3.613	3.141	0.96	5.29	6.13	3.87
4	198	3	3.979	3.233	0.94	8.78	7.34 (7.03)	4.53 (6.89)
5	45	5	1.583	2.945	1.17	1.30	3.38	2.75
6	72	5	2.040	3.019	1.10	2.39	4.31	3.24
7	127	5	2.319	3.318	1.09	4.71	5.43	4.04
8	198	5	2.710	3.370	1.06	8.00	6.63	4.71
9	45	11	1.626	3.159	1.18	1.67	3.65	3.01
10	72	11	2.069	3.146	1.11	3.01	4.63	3.52
11	127	11	2.444	3.234	1.07	5.85	5.91	4.29
12	198	11	3.025	3.414	1.03	10.4	7.36	5.06

[a] DP = degree of polymerization of the backbones based on ^{1}H-NMR analysis. [b] n = spacer length of the side chains. [c] Data from MBBA solutions at T = 25 °C.

Table 4. Hydrodynamic Parameters of Partially-Hydrosilated Side-Chain Liquid-Crystalline Polysiloxanes in 5OCB (T = 62 °C)

no.	DP[a]	n[b]	SiH content (%)[c]	$\eta°[\eta_{off}]$ (P·mL/g)	$\eta°[\eta_{on}]$ (P·mL/g)	$R_{\|}/R_{\perp}$	τ_r (μs)	$R_{h,off}$ (nm)	$R_{h,on}$ (nm)
12	198	11	<5	3.025	3.414	1.03	10.4	7.36	5.06
13	198	11	16	2.748	3.377	1.05	9.88	6.83	4.83
14	198	11	32	2.382	3.242	1.08	9.01	6.10	4.47
15	198	11	73	1.629	2.352	1.10	6.35	4.28	3.20

[a] DP = degree of polymerization of the backbones based on ^{1}H-NMR analysis. [b] n = spacer length of the side chains. [c] Percentage of unhydrosilated SiH.

application of the field is very small, we assume $[\eta_{off}] \sim [\eta_{on}] \sim [\eta_b]$ for LCP solutions in MBBA.

Turning now to the Brochard theory,[16] we find expressions for the increments in Miesowicz viscosities:

$$\delta\eta_c = \frac{ckT}{N}\left(\frac{R_{\|}^2}{R_{\perp}^2}\right)\tau_r \qquad (2)$$

and

$$\delta\eta_b = \frac{ckT}{N}\left(\frac{R_{\perp}^2}{R_{\|}^2}\right)\tau_r \qquad (3)$$

where $R_{\|}^2$ and $R_{\perp}^2$ are the rms end-to-end distances of the LCP measured parallel and perpendicular to the director, respectively, τ_r is the conformational relaxation time of the LCP, c is LCP concentration, and $N = M/N_A$ is the molecular mass of the LCP.

We first point out that eq 2 provides a straightforward rationale for our experimental observation[14,15] that main-chain LCPs, which have highly prolate conformations ($R_{\|} \gg R_{\perp}$), exhibit very large $[\eta_c]$, whereas side-chain LCPs, which have quasi-spherical conformations ($R_{\|} \sim R_{\perp}$), exhibit very small $[\eta_c]$. Taking the ratio of eqs 2 and 3, we obtain for the ratio of viscosity increments

$$\frac{\delta\eta_c}{\delta\eta_b} = \frac{R_{\|}^4}{R_{\perp}^4} \qquad (4)$$

For LCP solutions in 5OCB, we make the assignments $\eta_{on} = \eta_c$ and $\eta_{off} = \eta_b$, and hence, in Table 3, we list the limiting values of the specific viscosity increments for the various LCP/solvent systems, computed from the intrinsic viscosities as $\lim \delta\eta/c = \eta°[\eta]$, where $\eta°$ is the solvent viscosity, and the corresponding values of the ratio $R_{\|}/R_{\perp}$ computed via eq 4. The magnitude of the ER response is given by

$$\eta_{on} - \eta_{off} = \eta°_{on} - \eta°_{off} + c\left(\frac{\delta\eta_{on}}{c} - \frac{\delta\eta_{off}}{c}\right)$$
$$= \eta°_c - \eta°_b + c\left(\frac{\tau_r kT}{N}\right)\left(\frac{R_{\|}^2}{R_{\perp}^2} - \frac{R_{\perp}^2}{R_{\|}^2}\right) \qquad (5)$$

where $\eta°_{on}$ and $\eta°_{off}$ refer to the solvent values. From this equation, since $R_{\|}/R_{\perp}$ is known, we can now determine the molecular relaxation time, τ_r. These values are also given in Table 3. These results provide a molecular interpretation of our experimental observations. Thus, the relaxation time and the associated hydrodynamic volume have a relatively weak molecular weight dependence, $\tau_r \sim M^{1.25}$, smaller than that of a Gaussian chain, which is not surprising since so much of the mass is in the side chains. This, coupled with the fact that the chain anisotropy, $R_{\|}/R_{\perp}$, decreases with an increase of molecular weight and indeed for the two specimens of the n = 3 polymer of highest molecular weight $R_{\|}/R_{\perp}$ indicates a crossover from prolate to oblate shape, has the consequence of imparting a very weak molecular weight dependence to $\delta\eta_c$ and a strong molecular weight dependence to $\delta\eta_b$.

A similar analysis of the viscometric data in Figure 13, which shows the dependence of $[\eta_{on}]$ and $[\eta_{off}]$ on the side-chain density for the DP = 198, n = 3 polymer, is given in Table 4. These data show that $R_{\|}/R_{\perp}$ systematically increases, and the relaxation time τ_r systematically decreases with a decrease of side-chain density.

It is pertinent to point out that our observation that $[\eta_{on}] < [\eta_{off}]$ and hence, via the Einstein equation, that the ratio of effective hydrodynamic radii, $R_{h,on}/R_{h,off} < 1$, appears at first sight to be inconsistent with the conformational model of a prolate ellipsoid ($R_{\|} \geq R_{\perp}$), indicated by the Brochard theory for many of these

polymers. For an impermeable prolate ellipsoid in a simple shear flow, the maximum viscous energy dissipation, and hence the largest intrinsic viscosity, should occur when the major axis of the ellipsoid is along the shear gradient. The discrepancy arises because the Brochard model embodies anisotropic chain hydrodynamics, whereas the Einstein description has isotropic hydrodynamics. Thus, for an impermeable sphere ($R_{||} = R_{\perp} = R_h$), eq 4 predicts the viscosity increment associated with the addition of polymer should be the same for both η_b and η_c, i.e., $\delta\eta_b = \delta\eta_c$. However, application of the Einstein equation indicates the increment should be higher in the medium of higher viscosity, i.e., $\delta\eta_b = 2.5\eta_b^\circ V_h < \delta\eta_c = 2.5\eta_c^\circ V_h$, where $V_h = 4\pi R_h^3/3$ and where η_c° and η_b° are the solvent viscosities.

In MBBA, the situation should be similar to that in 5OCB when the field is off but will be quite different when the field is on, because the solvent has a negative $\Delta\epsilon$. Thus, application of the electric field has only a minor effect on the measured viscosity, $\eta_{on} \sim \eta_{off}$. We observe a small but reproducible negative ER effect, which means that the electric torque has a significant influence on the director orientation, but it is not clear whether the alignment is improved in the flow direction ($\eta_{on} \sim \eta_b$) or along the vorticity axis ($\eta_{on} \sim \eta_a$). Since the change in intrinsic viscosity is so small, i.e., $[\eta_{on}] \sim [\eta_{off}]$, and each has a similar molecular weight dependence, $[\eta_{on}] \sim [\eta_{off}] \sim M^{0.3}$ (Figure 12), the former situation seems more likely.

Conclusions

The electrorheological properties of nematic solutions of side-chain liquid-crystalline polysiloxanes are quite different in 5OCB, which has positive $\Delta\epsilon$, than in MBBA, which has negative $\Delta\epsilon$. In 5OCB, we find $[\eta_{on}] < [\eta_{off}]$, with $[\eta_{on}] \sim M^{0.1}$ and $[\eta_{off}] \sim M^{0.4}$. In MBBA, $[\eta_{off}] \sim [\eta_{on}] \sim M^{0.3}$. A further divergence is noted between the present observations in 5OCB and earlier studies[14] of main-chain LCPs in 5OCB where it was observed that $[\eta_{on}] \gg [\eta_{off}]$, with $[\eta_{on}] \sim M^{1.0}$ and $[\eta_{off}] \sim M^0$. These observations can be interpreted within the framework of the Brochard hydrodynamic model,[16] if we assume that the side-chain LCPs have a quasi-spherical conformation ($R_{||} \sim R_{\perp}$), whereas the main-chain LCPs have a highly prolate conformation ($R_{||} \gg R_{\perp}$). Thus, the difference in the ER response of side-chain and main-chain LCPs in nematic solvents with positive $\Delta\epsilon$ arises because the field orients the chain dimension $R_{||}$ along the shear gradient and $R_{||}$ rotates toward the flow direction when the field is turned off. For the end-on side-chain polysiloxane LCPs studied in this work, the fits to the Brochard model indicate a trend from slightly prolate to slightly oblate character as molecular weight and side-chain density increase or as spacer length decreases. The absence of a substantial ER effect for the side-chain LCPs in MBBA, which has negative $\Delta\epsilon$, arises because the chain dimension $R_{||}$ is oriented near the plane formed by the flow direction and vorticity axis both with the field on and with the field off.

Acknowledgment. Financial support from National Science Foundation Science and Technology Center ALCOM is gratefully acknowledged.

References and Notes

(1) Jordan, T. C.; Shaw, M. T. *IEEE Trans. Electr. Insul.* **1989**, *24*, 849.
(2) Halsey, T. C. *Science* **1992**, *258*, 761.
(3) Chandrasekhar, S. *Liquid Crystals*; Cambridge University Press: Cambridge, U.K., 1992.
(4) de Gennes, P.-G.; Prost, J. *The Physics of Liquid Crystals*, 2nd Ed.; Clarendon Press: Oxford, U.K., 1993.
(5) Carlsson, T.; Skarp, K. *Mol. Cryst. Liq. Cryst.* **1981**, *78*, 157.
(6) Skarp, K.; Carsson, T.; Lagerwall, S. T.; Stebler, B. *Mol. Cryst. Liq. Cryst.* **1981**, *66*, 199.
(7) Yang, I.-K.; Shine, A. D. *J. Rheol.* **1992**, *36*, 1079.
(8) Yang, I.-K.; Shine, A. D. *Macromolecules* **1993**, *26*, 1529.
(9) Clark, M. G.; Saunders, F. C.; Shanks, I. A.; Leslie, F. M. *Mol. Cryst. Liq. Cryst.* **1981**, *70*, 195.
(10) Carlsson, T.; Skarp, K. *Liq. Cryst.* **1986**, *1*, 455.
(11) Hongladarom, K.; Burghardt, W. R. *Macromolecules* **1993**, *26*, 785.
(12) Chow, A. W.; Hamlin, R. D.; Ylitalo, C. R. *Macromolecules* **1992**, *25*, 7135.
(13) Skarp, K.; Lagerwall, S. T.; Stebler, B. *Mol. Cryst. Liq. Cryst.* **1980**, *60*, 215.
(14) Chiang, Y.-C.; Jamieson, A. M.; Kawasumi, M.; Percec, V. *Macromolecules* **1997**, *30*, 1992.
(15) Chiang, Y.-C.; Jamieson, A. M.; Campbell, S.; Lin, Y.; O'Sidocky, N.; Chien, L. C.; Kawasumi, M.; Percec, V. *Rheol. Acta*, in press.
(16) Brochard, F. *J. Polym. Sci., Polym. Phys. Ed.* **1979**, *17*, 1367.
(17) Noirez, L.; Keller, P.; Cotton, J. P. *Liq. Cryst.* **1995**, *18*, 129.
(18) Gu, D.-F.; Jamieson, A. M.; Wang, S.-Q. *J. Rheol.* **1993**, *37*, 985.
(19) Apfel, M. N.; Finkelmann, H.; Janini, G. M.; Laub, R. J.; Lühmann, B.-H.; Price, A.; Roberts, W. L.; Shaw, T. J.; Smith, C. A. *Anal. Chem.* **1985**, *57*, 651.
(20) Marvel, C. S.; Garrison, W. E., Jr. *J. Am. Chem. Soc.* **1959**, *81*, 4737.
(21) Sauer, R. O.; Scheiber, W.; Brewer, S. D. *J. Am. Chem. Soc.* **1946**, *68*, 962.
(22) Percec, V.; Hahn, B. *Macromolecules* **1989**, *22*, 1588.
(23) Yilgor, I.; McGrath, J. E. *Adv. Polym. Sci.* **1986**, *86*, 1.
(24) Gray, G. W. In *Side-Chain Liquid-Crystalline Polymers*; McArdle, C. B., Ed.; Blackie: New York, 1989.
(25) Finkelmann, H.; Rehage, G. *Makromol. Chem., Rapid Commun.* **1980**, *1*, 733.
(26) Ringsdorf, H.; Schneller, A. *Makromol. Chem., Rapid Commun.* **1982**, *3*, 557.
(27) Gähwiller, Ch. *Mol. Cryst. Liq. Cryst.* **1973**, *20*, 301.
(28) Appelt, B.; Meyerhoff, G. *Macromolecules* **1980**, *13*, 657.
(29) Mather, P. T.; Pearson, D. S.; Larson, R. G. *Liq. Cryst.* **1996**, *20*, 527; *Liq. Cryst.* **1996**, *20*, 539.
(30) Han, H. W.; Rey, A. D. *J. Rheol.* **1995**, *39*, 301.
(31) Gu, D.-F.; Jamieson, A. M. *J. Rheol.* **1994**, *38*, 555.
(32) Carlsson, T. *Mol. Cryst. Liq. Cryst.* **1984**, *104*, 307.

MA970400F